Adsorption Configurations and Energetics of BCl_x ($x = 0-3$) on TiO_2 Anatase (101) and Rutile (110) Surfaces†

Jee-Gong Chang,*,‡ Jenghan Wang,§ and M. C. Lin§,||

National Center for High-Performance Computing, Number 28, Nan-Ke 3rd Road, Hsin-Shi, Tainan, Taiwan, Department of Chemistry, Emory University, Atlanta, Georgia 30322, and Center for Interdisciplinary Molecular Science, Institute of Molecular Science, National Chiao Tung University, Hsinchu, Taiwan 300

Received: December 26, 2006; In Final Form: March 13, 2007

This study investigates the adsorption and reactions of boron trichloride and its fragments (BCl_x) on the TiO_2 anatase (101) and rutile (110) surfaces by first-principles calculations. The results show that the possible absorbates on the TiO_2 anatase and rutile surfaces are very similar. The single- and double-site adsorption configurations are found for both anatase and rutile surfaces. The particular adsorbate feature on the anatase surface is its in-plane double-site adsorption by Ti and O from its sawtooth surface. The potential energy surface shows that BCl_3 can be adsorbed on the O site for both the anantase and rutile surfaces and the most of the BCl_x reaction on both anatase and rutile surfaces are endothermic, except for the dissociative reaction on the rutile surface. The energy levels of the BCl_x reactions between the anatase and rutile surfaces show that the rutile surface has lower energy levels than those of anatase surface. This result reveals that the BCl_x dissociative adsorption more easily occurs on rutile surface than on anatase surface.

Introduction

TiO_2 is a very versatile and robust material which has been employed for many industrial applications, such as photocatalysis[1,2] and solar energy conversion by means of photoelectrochemical water splitting[3] or photoelectric conversion by photovoltaics, which have been pioneered by Graetzel and coworkers[1,4−7] for their dye-sensitized solar cells using nanoparticle films of TiO_2. In that system, dye sensitizers are strongly bonded chemically with the TiO_2 substrate by the carboxyl group, −C(O)O−.

For a similar solar cell fabrication, we have succeeded in depositing InN thin films by OMCVD (organometallic chemical vapor deposition) on TiO_2 nanopaticles with HN_3 and trimethyl indium;[8] the results exhibit a broad UV/vis-absorption around 390−800 nm. To enhance the electron transfer from InN to TiO_2, various chemical linking groups[9,10] forming strong bonding between the sensitizer and the metal oxide substrate are being investigated. Among them, −B(O)O−, which may be produced by the reaction of BCl_x with TiO_2, is believed to have a rather strong binding with TiO_2 and may potentially bond with the N atom in the InN film. Practically, BCl_x species can be generated readily in plasma by microwave or radio frequency discharge, for example. B is a typical p-doping material in use by the semiconductor industry.

In this study, the binding configurations and energies of BCl_x ($x = 0-3$) on the most stable titania surfaces, anatase (101) and rutile (110), have been predicted by first-principles calculations. The result of the present study to be presented below indeed shows very strong bonding between BCl_x ($x < 3$) and TiO_2 on both surfaces. However, the potential energy surfaces show that the BCl_x dissociative reactions on both surfaces are mostly endothermic due to the strong B−Cl bonds.

Computational Model and Method

Figure 1a,b shows the structures of TiO_2 anatase (101) and rutile (110) surfaces. The larger gray atoms and smaller red atoms represent the Ti and O atoms, respectively. The anatase and rutile TiO_2 surfaces have similar structures in that both have the 2- and 3-fold-coordinated O atoms and 5- and 6-fold-coordinated Ti atoms, labeled as 2c-O, 3c-O, 5c-Ti and 6c-Ti, respectively. It has been shown that these two surfaces have lower energies with similar characteristics[11] and may coexist in nanoparticle films. The 2-fold-coordinated O and 5-fold-coordniated Ti atoms are more active because the lower-coordination of these atoms bind more strongly with adsorbates.

The slab model is adopted to simulate the interaction between the TiO_2 surface and BCl_x species. The super cells employed for both TiO_2 anatase and rutile calculations contain 16 [TiO_2] units. In the direction perpendicular to the super cell, a vacuum space is imposed for the surface reaction as well as to ensure no interaction with the lowest layer of the upper slab. The lowest layer of the super cell is fixed in calculation to prevent surface deformation.

The geometrical structures are optimized by Vienna ab initio Simulation Package (VASP),[12−15] implementing the density functional theory. The generalized gradient approximation (GGA)[16,17] used for the total energy calculations is that of Perdew−Wang 1991 (PW91) formulation.[16] The core pseudopotentials supplied by VASP are used for the present calculation. The ten 3p, 3d, and 4s electrons of each Ti atom and the six 2s and 2p electrons of each O atom are explicitly considered. For the periodic condition, the electronic orbitals are expanded by a plane-wave basis set. The plane wave expansion includes all plane waves with their kinetic energies smaller than the chosen cutoff energy, $\hbar K^2/2m < E_{cut}$, which ensures the convergence

† Part of the special issue "M. C. Lin Festschrift".

* Corresponding author. Currently Emerson Center Visiting Fellow at Emory University. E-mail: changjg@nchc.org.tw

‡ National Center for High-Performance Computing.

§ Emory University.

|| National Chiao Tung University.

10.1021/jp0689363 CCC: $37.00
Published on Web 04/21/2007

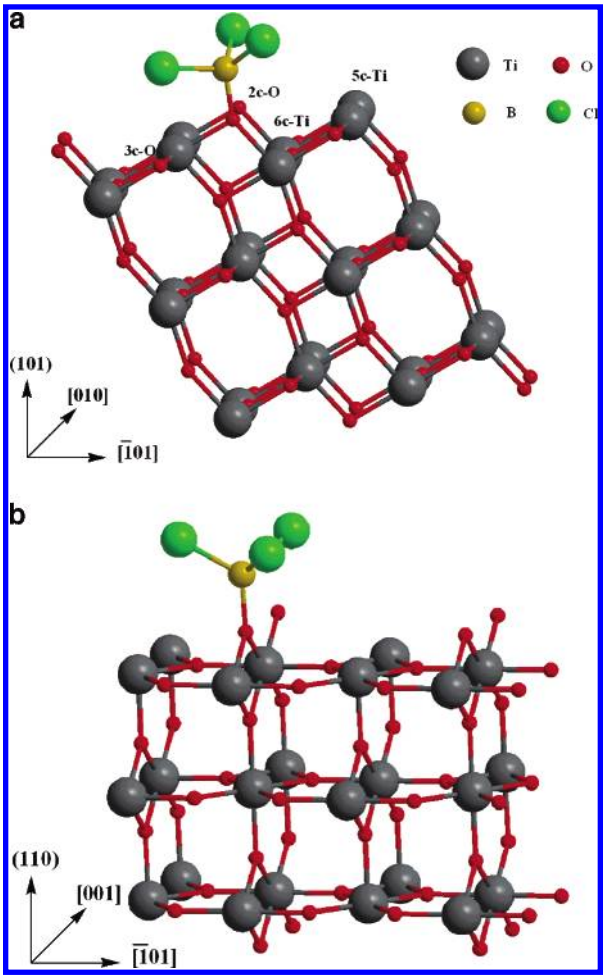

Figure 1. Geometry model for TiO2 (a) anatase (101) and (b) rutile (110) surfaces.

with respect to the basis set. The Brillouin zone is sampled with the chosen Monkhorst-Pack[18] *k*-points, which also ensures the convergence of the whole system.

Results and Discussion

a. Verification. Verifications on the correctness and accuracy of the model adopted herein have been carried out. The bulk properties and adsorption reactions for both TiO_2 anatase and rutile surfaces are computed to verify the calculation parameters. The model size $3 \times 2 \times 1$ is adopted along the three primitive vector directions for anatase, the Monkhorst-Pack *k*-points is set as $1 \times 2 \times 2$, and the E_{cut} set as 600 eV. The lattice constant obtained for the anatase crystal are $a = 3.805$ Å and $c = 9.798$ Å, which agree well with the X-ray diffraction results of $a = 3.785$ Å and $c = 9.514$ Å.[19] The lattice constant obtained from the bulk calculation is applied to the surface models with a 10 Å vacuum space. The adsorption energy of water on TiO_2(101) was predicted to be 14.3 kcal/mol, which falls in the experimental range, 11.5−16.1 kcal/mol.[20]

Similarly, the model size of $1 \times 2 \times 2$ along the three primitive vectors is adopted for the TiO_2 rutile structure. The Monkhorst-Pack *k*-points is set as $3 \times 3 \times 2$, and the value of $E_{cut}$is set as 600 eV. The lattice constant obtained for the rutile crystal found are $a = 4.659$ Å and $c = 2.985$ Å, which agree well with the X-ray diffraction results of $a = 4.593$ Å and $c = 2.933$ Å.[21] The adsorption energy of H_2O on the 5c-Ti was predicted to be 18.4 kcal/mol, which also agrees well with the literature value of 20.9 kcal/mol.[22,23] Finally, the bond length of the gas-phase molecule of BCl_3 and its fragments are calculated by VASP and compared to the results calculated by Gaussian03[24] as listed in Table 1 for comparison. It is shown that the results obtained by VASP agree well with those obtained by Gaussian03.

TABLE 1: Comparison of Bond Length and Bond Angle for BClx, $x = 1-3$, Calculated by VASP and Gaussian 03

	r(B−Cl1)	*r*(B−Cl2)	*r*(B−Cl3)	−ClBCl
BCl_3	1.747, 1.753[a]	1.747, 1.753[a]	1.747, 1.753[a]	120.1, 120.0[a]
BCl_2	1.716, 1.737[a]	1.716, 1.737[a]		127.1, 125.6[a]
BCl	1.723, 1.733[a]			

[a] B3LYP/6-31+G(d).

b. Adsorbate Structures on Anatase Surface. The possible adsorption configurations of BCl_3 and its fragments on the TiO_2 anatase (101) surface are shown in Figure 2, and the associated bond lengths and adsorption energies are also listed in Table 2. The adsorbates on the 5-fold-coordinated Ti atoms or the 2-fold-coordinated O atoms are labeled as adsorbate-Ti and adsorbate-O. In Table 2, the two-site adsorbates on either O and O or Ti and O are also included besides the single-site adsorbate on Ti or O. The most stable adsorbate structure for the single-site adsorption configuration is $Cl_2B-O(a)$ with the adsorption energy of 81.6 kcal/mol and the B−O bond length of 1.341 Å, which is the shortest bond length among the single-site adsorbates. For the same adsorbate on Ti, $Cl_2B-Ti(a)$, the adsorption energy is only 9.0 kcal/mol, which is far less than that of $Cl_2B-O(a)$. In addition, for the $Cl_2B-Ti(a)$ adsorbate, the B−Ti bond length is 2.766 Å, which is much larger than that of $Cl_2B-O(a)$. The adsorbates with stronger adsorption energies between B and O atoms than that of B and Ti atoms resulted from the empty p-orbital of B atom, which interacts strongly with the lone pair electrons of the O atom. Similarly, the BCl_3 gas molecule can only adsorb on the surface O rather than on Ti atoms. One of the three bond lengths of the BCl_3 adsorbate structure is longer than the other two, i.e., r(B−Cl3) > r(B−Cl2) > r(B−Cl); see Table 2. This indicates that the bonding between the third Cl and B atoms is weaker than the other two Cl−B because the B atom is more stable at its 3-fold coordinated.

Five double-site adsorbates are found in the calculation. Two of them are B and BCl, adsorbed on both Ti and O sites on the same (010) plane producing B(Ti)O(a) and ClB(Ti)O(a), respectively. The other two are BCl and BCl_2, which adsorb across two O sites on two neighboring (010) planes, forming bridge structures ClB(O)O′(a) and $Cl_2B(O)O'(a)$, respectively. The fifth involves BCl, which adsorbs across a Ti and an O′ site forming a double-site adsorbate, ClB(Ti)O′(a). The adsorption sites of Ti and O located in the same (010) plane will be called in-plane Ti and O herein, as in the former two double-site adsorption configurations. The latter three double-site adsorption configurations, having their adsorption sites located at different (010) planes, will be called bridge Ti and O′ here (see Figure 1 for the structures). The adsorption energies for the former two adsorbates on in-plane Ti and O, B(Ti)O(a) and ClB(Ti)O(a), are 101.2 and 61.0 kcal/mol. Similarly, the adsorption energies for the bridge O site adsorbates, ClB(O)-O′(a) and $Cl_2B(O)O'(a)$, and adsorbate ClB(Ti)O′(a) for the bridge Ti and O site are 84.2, 78.7, and 39.7 kcal/mol, respectively. The adsorbates of double-site adsorption, either on Ti and O or on O and O′, are relatively more stable than the same adsorbates of single-site adsorption. For example, the adsorption energies of double-site adsorbate of BCl, ClB(Ti)O-(a) adsorbed on either in-plane or bridge Ti and O′ and ClB-

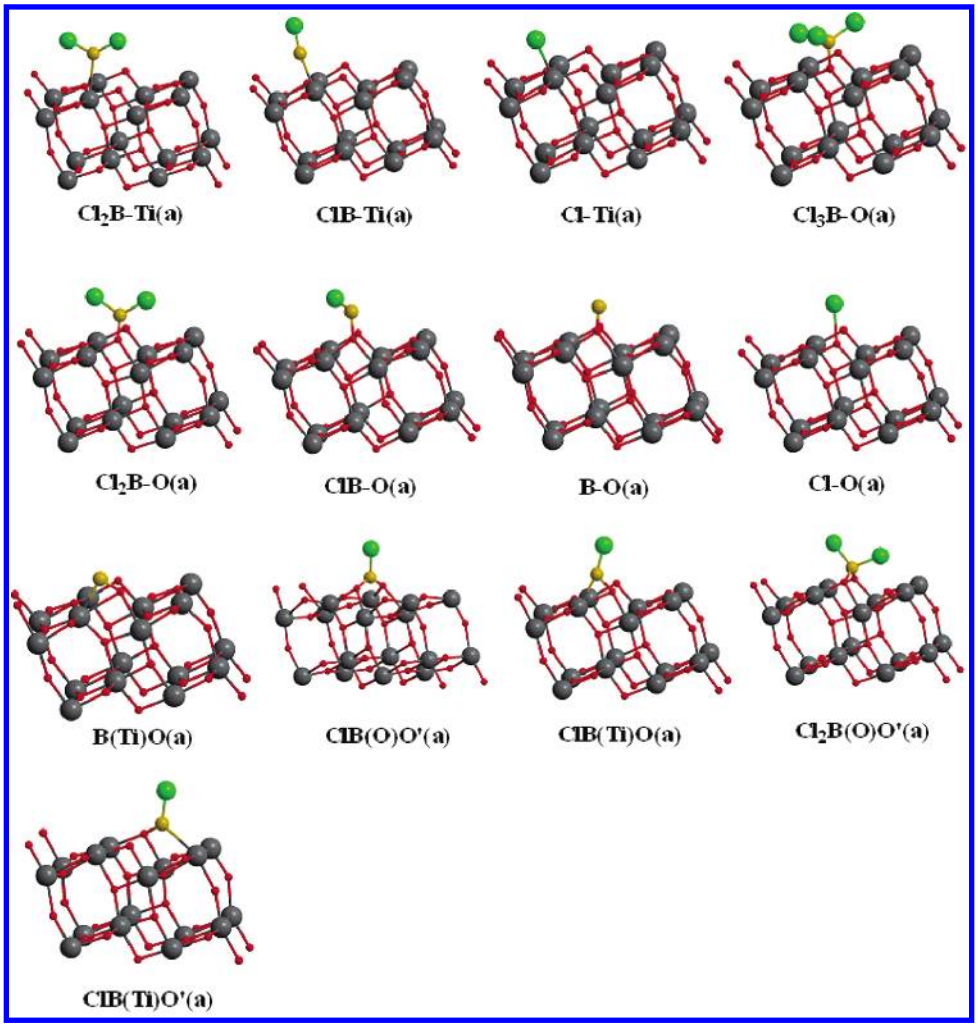

Figure 2. Possible adsorbate on TiO_2 anatase (101) surface.

TABLE 2: Bond Length and Adsorption Energy of Possible Adsorbate on TiO_2 Anatase (101) Surface

	r(Ti(O)−B(Cl))	r(B−Cl1)	r(B−Cl2)	r(B−Cl3)	E_{ads}
Cl_2B−Ti(a)	2.766	1.707	1.707		9.0
ClB−Ti(a)	2.379	1.680			14.8
Cl_3B−O(a)	1.460	1.776	1.808	2.076	8.4
Cl_2B−O(a)	1.341	1.771	1.751		81.6
ClB−O(a)	1.469	1.825			11.9
B−O(a)	1.281				97.8
Cl−Ti(a)	2.374				17.0
Cl−O(a)	2.260				2.7
B(Ti)O(a)	2.299, 1.238				101.2
ClB(Ti)O(a)	2.210, 1.328	1.734			61.0
ClB−(O)O′(a)	1.375, 1.384	1.775			84.2
Cl_2B−(O)O′(a)	1.469, 1.475	1.871	1.924		78.7
ClB(Ti)O′(a)	2.689, 1.364	1.758			39.7

(O)O′(a), are larger than those of single-site adsorbates, ClB−Ti(a) and ClB−O(a), as indicated in Table 1. Similarly, the adsorption energy of the double-site adsorbate of the B atom, B(Ti)O(a), is also larger than that of single-site adsorbate, B−O(a), by 3.4 kcal/mol. The only one exception is Cl_2B(a), whose double-site adsorbate Cl_2B(O)O′(a) is less stable than the single-site adsorbate Cl_2B−O(a). This is because the 3-fold-coordinated B atom in Cl_2B−O(a) has a larger adsorption energy than that of the over-coordinated bonding configuration, Cl_2B-(O)O′(a).

Panels a and b of Figure 3 show the detailed structures of B(Ti)O(a) and ClB(Ti)O(a), respectively. For B(Ti)O(a), the B−Ti bond, 2.299 Å, is slightly longer than that of B−O bond, 1.238 Å. This again reflects that the B atom is adsorbed more preferably on the O than on the Ti atoms, as mentioned previously. In addition, the surface structure of TiO_2 also shows the influence by the B adsorbate that the bond lengths for O1−Ti1 and O1−Ti2 are stretched significantly, from 1.859 and 1.837 Å to 2.223 and 2.506 Å, respectively. The −Ti1O1Ti2 becomes smaller from 100.6° to 85.1°, and −Ti2O2Ti1 becomes larger from 94.8° to 115.0°, comparing to those of the bare TiO_2 surface. The adsorbate structure of ClB(Ti)O(a) is similar to B(Ti)O(a), where the B−O bond is also shorter than B−Ti. The length of the B−Cl bond is 1.734 Å, which is somewhat smaller than the B−Cl bonds of the equilibrium BCl_3 in the gas phase, 1.747 Å, and longer than that of the equilibrium BCl, 1.723 Å. This result indicates that the bond strength of B−Cl in adsorbate ClB(O)O′(a) lies in between those of BCl and BCl_3 in the gas phase. The influence of the TiO_2 structure by the adsorption of BCl is also similar to the B(a) case, except that effect exerted on O1 and Ti2 is slightly smaller than that by the B atom. This can be seen from the bond lengths of Ti1−O1 and Ti2−O1 for the BCl(a), which are shorter than those of B(a), and −Ti2O1Ti2 for BCl(a) is larger than that of B(a). Finally, the angle of −Ti2BO1 is 69.5° for BCl(a), which is smaller than that of −Ti2BO1, 84.5°, for the B(a) case.

Similarly, panels a and b of Figure 4 show the detailed structures of the double-site adsorbates, ClB(O)O′(a), and Cl_2B-

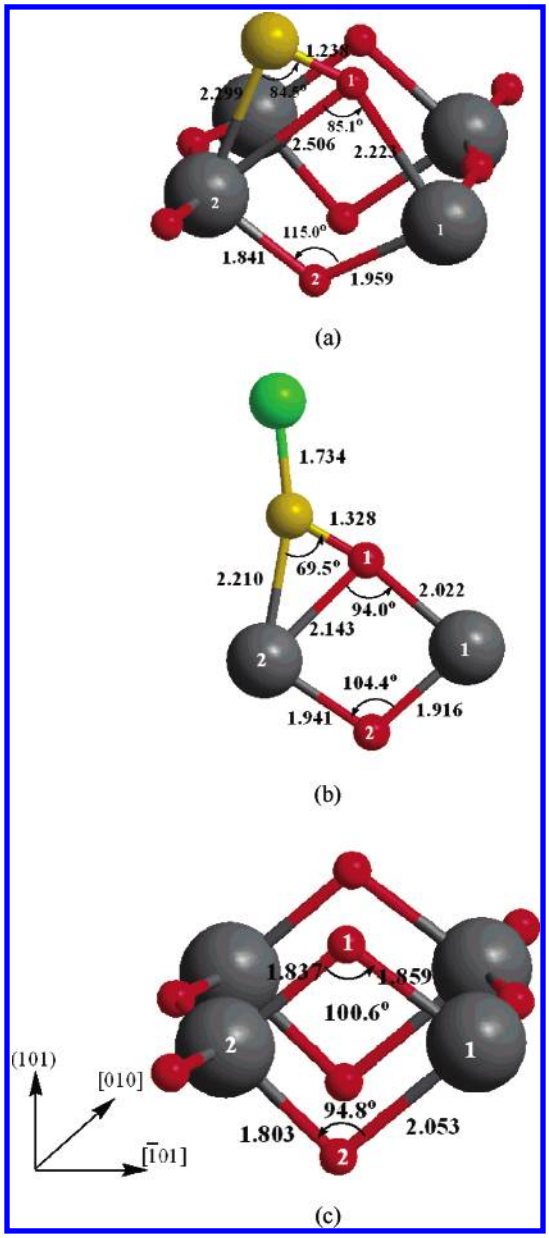

Figure 3. Detailed structure of (a) B(Ti)O(a), (b) ClB(Ti)O(a), and (c) bare TiO_2 anatase surface.

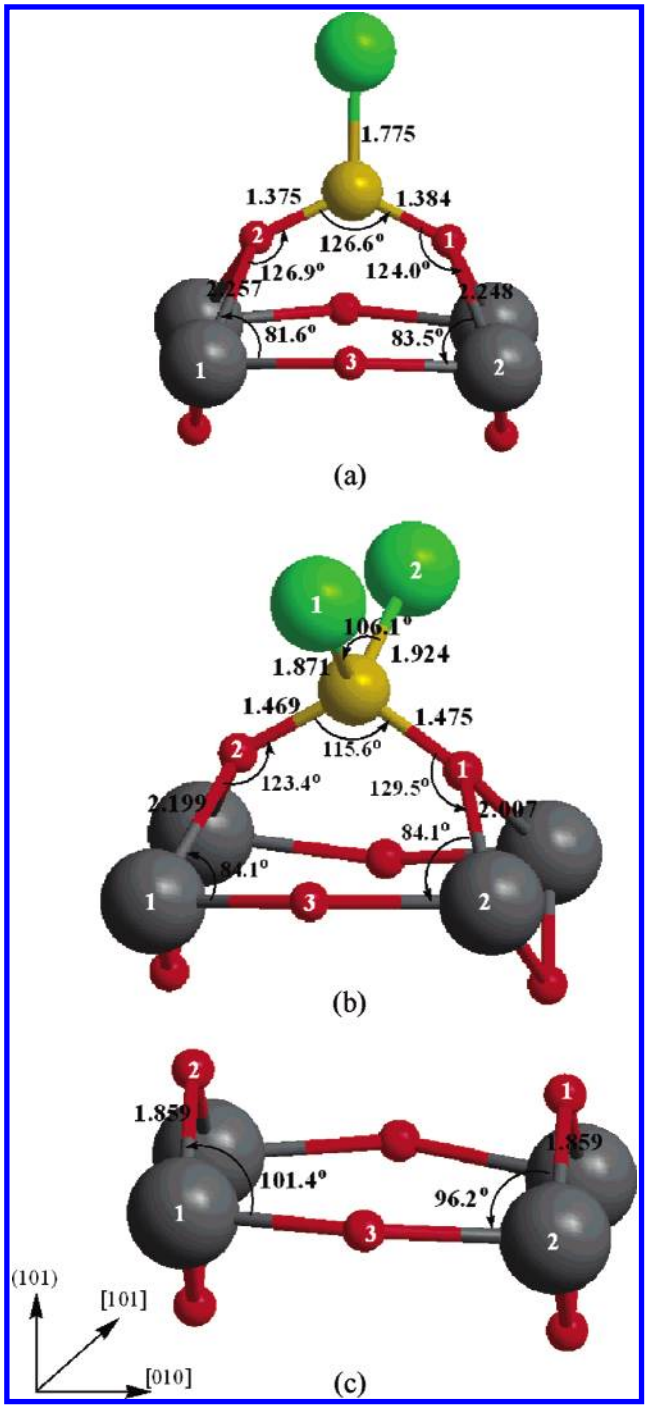

Figure 4. Detailed structure of (a) ClB(O)O′ (a), (b) $Cl_2B(O)O'$ (b), and (c) bare TiO_2 anatase surface.

(O)O′(a). For ClB−O(a), the two bond lengths between B and O atoms, B−O1 and B−O2, are 1.384 and 1.375 Å, respectively. The B−Cl bond is 1.775 Å, and −O1BO2 is 126.6°. The angle of two bridge O are bent inward from an equilibrium angle of 101.4° to 81.6°, −O2Ti1O3, at the left side in the figure, and from 96.2° to 83.5°, −O1Ti2O3, at the right side in the figure, respectively. The distance between these two bridge O atoms, O1−O2, is shorten to 2.464 Å by the binding force of B and 2O. The original distance between these two bridge O atoms is 3.785 Å on the bare surface. In addition, for the TiO_2 substrate, O2−Ti1 is also stretched from the equilibrium bond length of 1.859 to 2.257 Å, at left side in the figure, and the O1−Ti2 bond length is also stretched from 1.859 to 2.248 Å at right side in the figure.

For $Cl_2B(O)O'$(a) (see Figure 4b), the bond lengths of the B atom with the two adsorbed O atoms, B−O1 and B−O2, are 1.475 and 1.469 Å, and those of BCl1 and BCl2 are 1.871 and 1.924 Å, respectively. The angle between B and two O-atom adsorbent −O1BO2 is 115.6°. In addition, the distance between the two bridge O sites becomes 2.491 Å, which is considerably shorter than its original distance between the two bridge atoms, 3.785 Å, on the TiO_2 bare surface. Comparing the structures of $Cl_2B(O)O'$(a) and ClB(O)O′(a), all the bond lengths in the former are longer than those in the latter; and the distances between the two adsorption O sites of Cl_2B-(O)O′(a) are also longer than those of ClB(O)O′(a). This again reveals that the 3-fold-coordinated B atom has a stronger bonding force than that of 4-fold-coordinated ones. Similar to ClB(O)O′(a), all the bond lengths between Ti and O atom are also stretched by Cl_2B; however, the bond length is slightly shorter than those in ClB(O)O′(a). Finally, the angles of −O2Ti1O3 and −O1Ti2O3 are both equal to 84.1°, which are

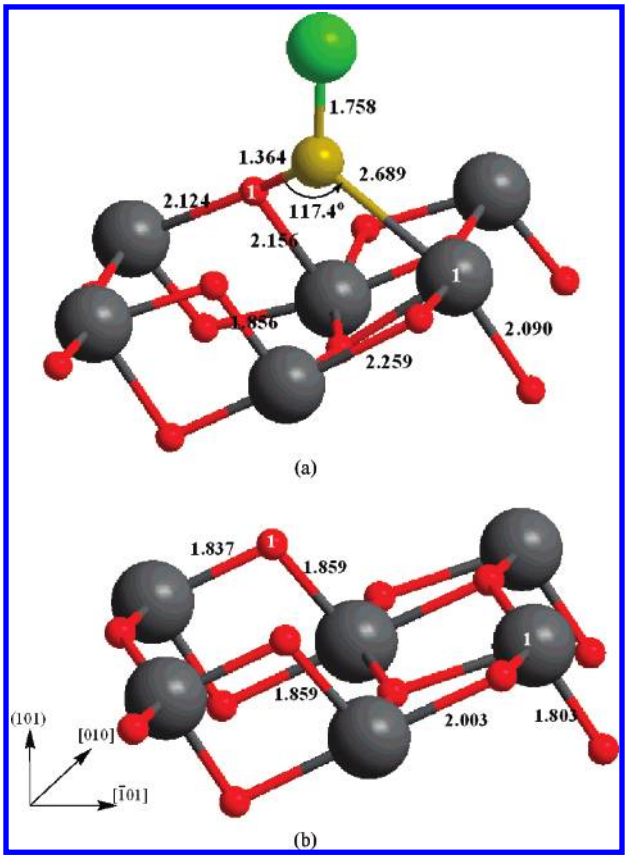

Figure 5. Detailed structure of (a) ClB(Ti)O′ (a) and (b) bare TiO_2 anatase surface.

larger than those of the related angles in ClB(a), 81.6° and 83.5°, respectively.

Figure 5 shows the detailed configuration of BCl adsorbed on the bridge O′ and Ti atoms, ClB(Ti)O′(a). The B−Ti bond is 2.689 Å, the B−O bond is 1.364 Å, and −O1BTi1 is 117.4°. Both of B−Ti and B−O bonds are longer than those B(Ti)O-(a) and ClB(Ti)O(a), where the adsorption sites, Ti and O, are located at in-plane positions. This is because the adsorption geometry for ClB(Ti)O′(a) is more constrained than those in B(Ti)O(a) and ClB(Ti)O(a). This is also the reason why the adsorption energy of ClB(Ti)O′(a) on bridge Ti and O is smaller than those of B(Ti)O(a) and ClB(Ti)O(a) on in-plane Ti and O. The O1−Ti1 with 3.530 Å in ClB(Ti)O′(a) adsorbed on bridge Ti and O′ has been shortened by 0.49 Å compared to the O1−Ti1 on the bare TiO_2 surface, 4.020 Å.

Finally, the adsorption energies for the Cl adsorbate on Ti and O sites, Cl−Ti(a) and Cl−O(a), are 17.0 and 2.7 kcal/mol and their bond lengths are 2.374 and 2.260 Å, respectively. Thus, the Cl atom adsorbs more preferably on the Ti atom than on the O atom. This is because the Cl atom prefers to donate the lone pair electron to Ti than to the electron-rich O site.

c. Adsorbate Structure on Rutile Surface. The possible adsorbate structures of BCl_3 and its fragments on the rutile (110) surface are shown in Figure 6, and the related bond lengths and adsorption energies are listed in Table 3. Similar to the results for adsorption on the anatase (101) surface presented above, both single-site and double-site adsorption structures are also found on the rutile surface. Among single-site adsorbates, Cl_2B−O(a) is the most stable, with an adsorption energy of 103.8 kcal/mol and a B−O bond length of 1.354 Å. In addition, similar to that on the anatase surface,

TABLE 3: Bond Length and Adsorption Energy of Possible Adsorbate on TiO_2 Rutile (110) Surface

	r(Ti(O)−B(Cl))	r(B−Cl1)	r(B−Cl2)	r(B−Cl3)	E_{ads}
Cl_2B−Ti(a)	2.951	1.687	1.688		9.2
ClB−Ti(a)	2.305	1.661			20.5
Cl_3B−O(a)	1.462	1.846	1.874	1.874	8.7
Cl_2B−O(a)	1.354	1.763	1.755		103.8
ClB−O(a)	1.214	1.661			78.5
B−Ti(a)	2.411				21.6
B−O(a)	1.292				121.3
Cl−Ti(a)	2.198				31.9
Cl−O(a)	1.677				17.3
ClB(O)O(a)	1.385, 1.385	1.760			124.8
Cl_2B(O)O(a)	1.542, 1.542	1.821	1.821		92.8
ClB(Ti)O′(a)	2.469, 1.324	1.735			70.7

the BCl_3 molecule can directly adsorb on an O atom. The adsorption energy of Cl_3B−O(a) is 8.7 kcal/mol, which is slightly larger than that of Cl_3B−O(a) on the anatase surface. The B−O is 1.462 Å, and the B−Cl1, B−Cl2, and B−Cl3 bonds are almost equal to 1.8 Å. This is different from Cl_3B−O(a) on the anatase surface, in which one of its B−Cl1 bonds is shorter than the other two due to the stronger interaction of the particular Cl1 atom than the other two Cl2 and Cl3 atoms (Table 2), showing that the three Cl atoms are not homogenously adsorbed on the B. This reveals that the O site on the rutile surface is more reactive than the same O site on the anatase surface.

The other single-site adsorbates involve B and Cl on Ti and O atoms, giving B−Ti(a), B−O(a), Cl−Ti(a), and Cl−O(a). The predicted adsorption energies show that B preferably adsorbs on the O rather than the Ti sites. Their adsorption energies are 121.3 kcal/mol for B−O(a) and 21.6 kcal/mol for B−Ti(a). This trend is similar to that observed on the anatase surface. Finally, the adsorption energies for the Cl atom on the Ti and O atoms are 31.9 and 17.3 kcal/mol, respectively. These are similar to the results on the anatase surface as aforementioned.

There are three adsorbates with double-site adsorption found for BCl and BCl_2 on the bridge O atoms, ClB(O)O(a) and Cl_2B-(O)O(a), and BCl on the bridge Ti and O atoms, ClB(Ti)O′(a). The adsorbates of ClB(O)O(a) and Cl_2B(O)O(a) have 124.8 and 92.8 kcal/mol adsorption energies, respectively, are located on the same ($\bar{1}01$) plane, whereas the adsorbate ClB(Ti)O′(a) with 70.7 kcal/mol adsorption energy is located on different ($\bar{1}01$) planes. Among three double-site adsorbates, ClB(Ti)O′(a) is the smallest. The trend of the adsorption energies is similar to that on the anatase surface, more energy is required to overcome the geometry constraint arising from long separation between the Ti and O sites.

Figure 7(a) and 7(b) show the adsorbate structures of ClB and Cl_2B on TiO_2 rutile (110). The bond lengths between B and the two bridge O atoms in ClB(O)O(a) are 1.385 Å and that in Cl_2B(O)O(a) is 1.542 Å. In addition, B−Cl is 1.760 Å in ClB(O)O(a) and is 1.821 Å in Cl_2B(O)O(a). The angle between B and two bridge O is predicted to be 116.8° in ClB-(O)O(a) and is 106.4° in Cl_2B(O)O(a). In addition, the bond lengths between Ti1 and O1 are 2.162 and 1.988 Å for ClB(a) and ClB_2(a), respectively. The Ti1−O1 in ClB(a) being smaller than that in Cl_2B(a), the B−O1 in ClB(O)O(a) being smaller than that in Cl_2B(O)O(a), and the −O1BO2 in ClB(a) being larger than that in Cl_2B(a) reflects that BCl(a) has a stronger bonding force.

Figure 8 shows the adsorbate structure of ClB(Ti)O′(a) on the TiO_2 rutile surface and the bare surface for comparison. The computed B−Ti and B−O are 2.469 Å and 1.324 Å,

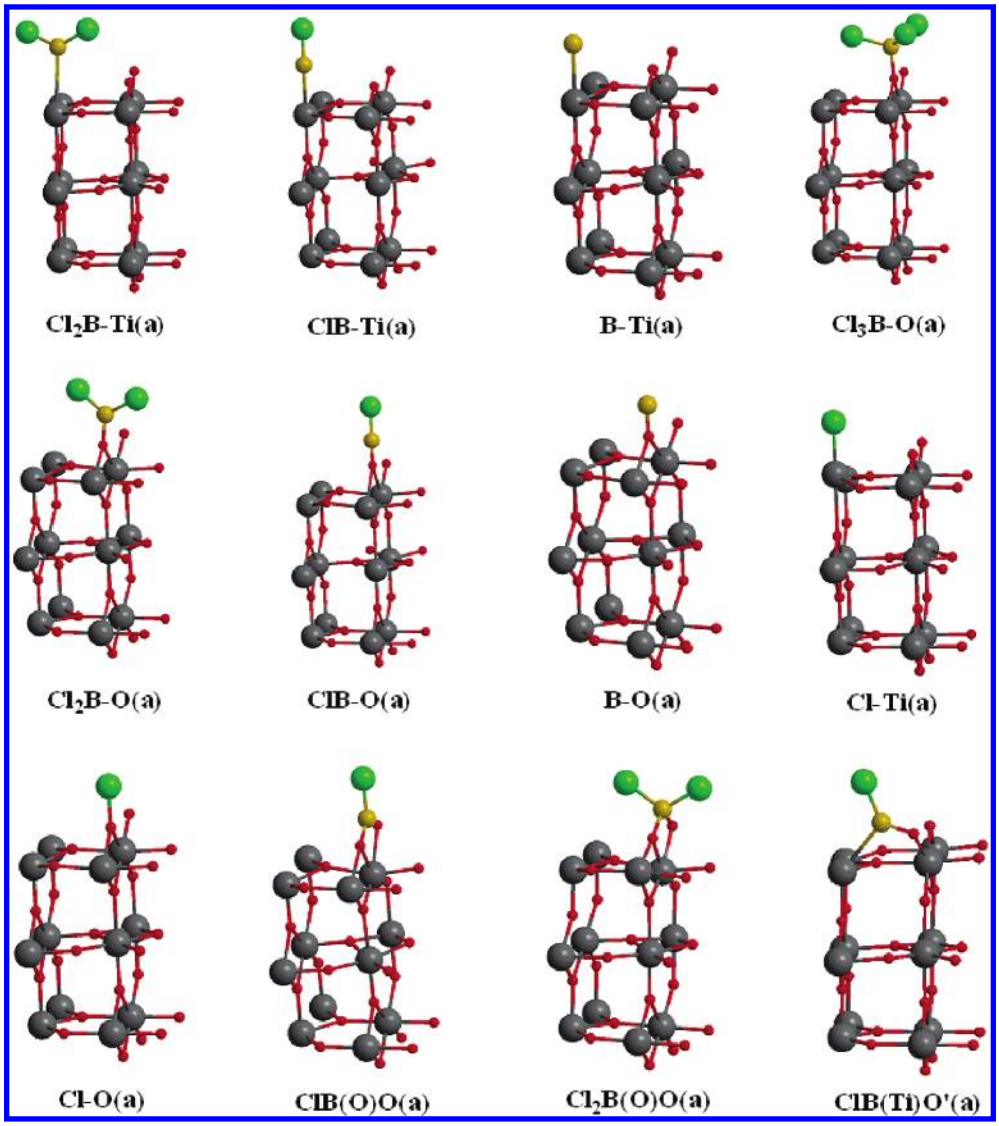

Figure 6. Possible adsorbate on TiO_2 rutile (110) surface.

respectively. The B−Cl and −Ti2BO1 in ClB(a) are 1.735 Å and 109.7°, respectively. The structure change of the TiO_2 surface shows that the surface O site is bent inward to form ClB(Ti)O′(a). The −O1Ti1O2 is changed from 90.4° to 79.3°. The original distance of O1−T2 is shortened from 3.563 to 3.171 Å due to the binding forces of B−O and B−Ti. Finally, the change of Ti1−O1 also reveals that the bridge O atom is slightly pulled up by bonding between B and O. The Ti1−O1 bond length is changed from 1.843 Å of the bare surface to 2.139 Å in the ClB(Ti)O(a).

d. Potential Energy Diagram BCl_x Adsorbates on Anatase Surface. Figure 9a shows the potential energy diagram for the dissociative adsorption of BCl_x, $x = 1-3$, on the anatase surface. The adsorption energies are similar to BCl_3(g) and the TiO_2 anatase (101) surface. The dissociative adsorption of BCl_3 on the surface is highly endothermic, except for the initial molecular adsorption of BCl_3(a). There are two possible dissociation pathways from BCl_3(a), producing Cl_2B−O(a) or Cl_2B(O)O′(a). As discussed above, the latter is less stable than the former. The dissociated Cl atom can be adsorbed on either Ti or O atoms. The dissociated adsorbates of Cl_2B−O(a) + Cl−Ti(a) are formed with the lowest energy of 25.8 kcal/mol.

Following the second Cl dissociation from BCl_2, the energy level is elevated because more energy is required to dissociate the second B−Cl bond, which is not compensated by the increase in the adsorption energy of BCl and the additional adsorption energy of the Cl atom. There are three double-site adsorptions of BCl, ClB(Ti)O(a) adsorbed on either in-plane or bridge, Ti and O, ClB(O)O′(a), as alluded to before and similar to the previous case, the dissociated Cl can be adsorbed on either Ti or O atoms. Thus, in total there are three possibilities for adsorption of the two dissociated Cl atoms: on two Ti, Ti and O, and two O atoms. From the three double-site adsorbates, there are in total nine different energy products. Among these nine dissociated states, the energetically most stable one is the ClB(a) doubly adsorbed on bridge O atoms, with the two dissociated Cl atoms individually adsorbed on two Ti sites, ClB-(O)O′(a) + 2Cl-Ti(a); its adsorption energy is 89.2 kcal/mol above BCl_3(g) + anatase (101). The next lowest state is BCl(a) doubly adsorbed on the O atoms with the two Cl atoms adsorbing on O and Ti sites individually. The adsorption energy of this adsorbate is 104.1 kcal/mol. Finally, the third lowest state (+112.5 kcla/mol) is the two dissociated Cl adsorbing on both two O sites. Other higher energy adsorbates, or less stable dissociative products, are given in Figure 9a.

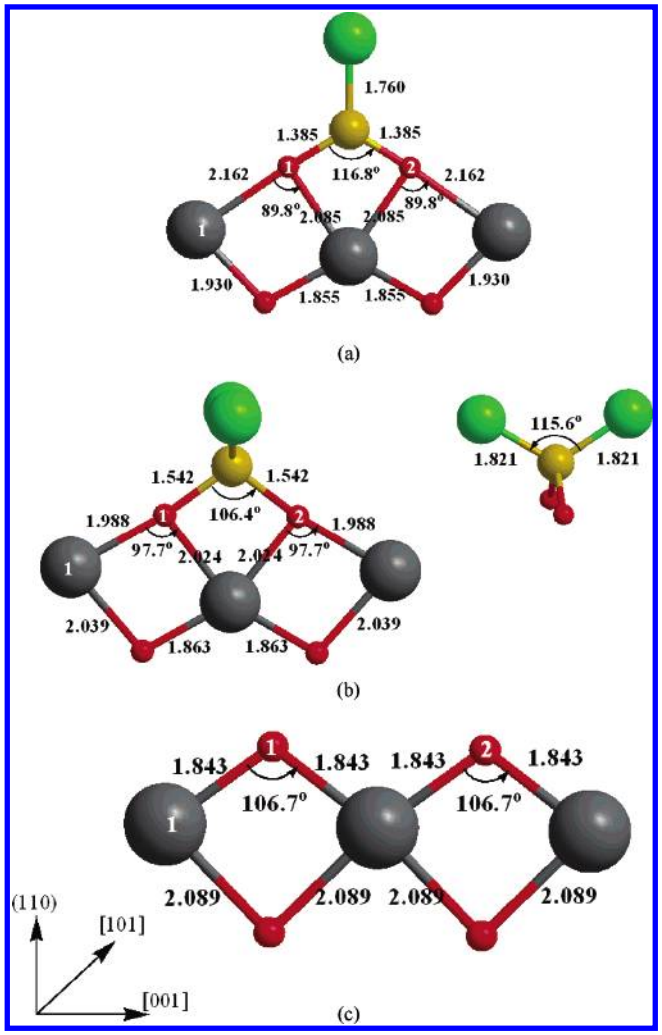

Figure 7. Detailed structure of (a) ClB(O)O(a), (b) $Cl_2B(O)O(a)$, and (c) bare TiO_2 rutile surface.

e. Potential Energy Diagram of Adsorbates on Rutile Surface. Similarly, Figure 9b shows the potential energy diagram of $BCl_x(a)$ on the TiO_2 rutile (110) surface. As in the anatase surface, the dissociative adsorption of BCl_3 on the rutile surface is also highly endothermic; however, the energies for the dissociation of the second and third Cl atoms are not so high as the analogous reactions on the anatase surface. In addition, the initial adsorption of $Cl_3B(a)$ on an O site, giving $Cl_3B-O(a)$, and its dissociation products of $Cl_2B-O(a)+Cl-Ti(a)$ are exothermic. These two energies are −8.7 and −10.8 kcal/mol, respectively.

Unlike the anatase case, only two adsorbates, ClB(O)O(a) and ClB(Ti)O′(a), are formed from the dissociation of $Cl_2B-O(a)$. Thus, six different products could be formed with the two dissociated Cl atoms adsorbing on either Ti or O atoms. Among these products, the most stable one is the BCl(a) adsorbed on the bridge O atoms with the two dissociated Cl atoms individually adsorbing on Ti atoms, ClB(O)O(a) + 2Cl-Ti(a). The total energy of these products is 19.9 kcal/mol above the reactants, $BCl_3(g)$ + rutile (110) surface.

f. Overall Comparison for BCl_3 Reaction on the Anatase and Rutile Surface. In terms of adsorption configurations, there are very similar adsorbates on both the TiO_2 anatase and rutile surfaces. For single site adsorbates on anatase and rutile surfaces, the slight difference is found, in which B atom can be weakly adsorbed on Ti atom forming B−Ti(a) on the rutile surface, though not on the anatase surface. This results from their structure characteristics of the sawtooth-anatase surface with the 2-fold-coordinated O and 5-fold-coordinated Ti and the flat-rutile surface with 2-fold-coordinated and 5-fold-coordinated Ti.[11] On the anatase surface, the O and Ti site are close (∼1.8 Å) and at the in-plane position so that the B cannot singly adsorbed on only Ti atom without the influence of the strong adsorption by the O atom. On the rutile surface, the O and Ti sites are rather far away (3.6 Å); therefore, B can be adsorbed on the Ti atom without the strong influence of by the neighboring O atom. Furthermore, the difference in double-site adsorptions between the anatase and rutile surfaces is similar. There are five double-site adsorbates found for the anatase surface and only three for rutile surface. The additional two double-site adsorbates of B(Ti)O(a) and ClB(Ti)O(a) for the anatase are due to the two very close Ti and O sites located at in-plane positions, where B and BCl can easily be adsorbed on these in-plane Ti and O atoms, as indicated above for the B atom adsorption.

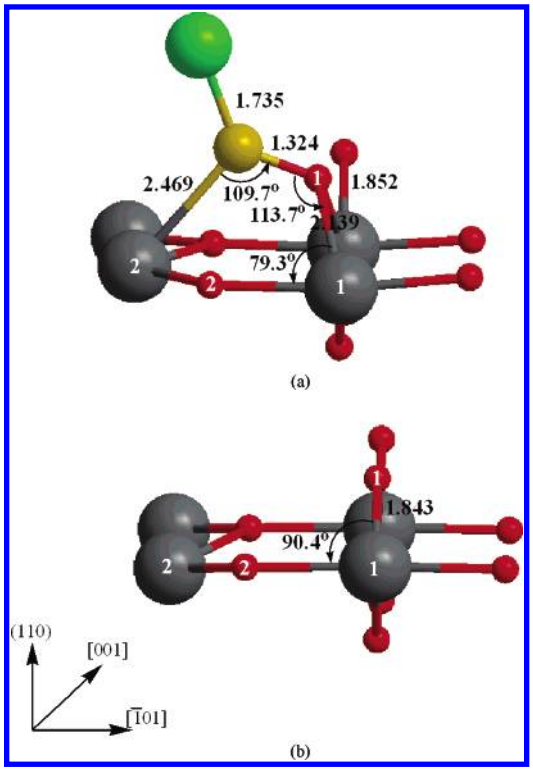

Figure 8. Detailed structure of (a) ClB(Ti)O′(a) and (b) bare TiO_2 rutile surface.

Comparing with the adsorption energies of all the adsorbates for both anatase and rutile surfaces, the B atom is adsorbed more preferably on the O than Ti atoms. On the other hand, Cl atom is more preferably adsorbed on the Ti atom. Comparing adsorption energy of the single-site adsorbate, both O and Ti sites of rutile are more active than those of anatase attributable to the difference in surface structures.

Finally, both potential energy surfaces show that BCl_3 can adsorb on the O site of both anantase and rutile surfaces, and most of the BCl_x fragments behave similarly. The dissociative adsorptions of BCl_3, on both surfaces are endothermic, except only for one reaction involving BCl_3 and rutile. Comparing the energetics of the BCl_x reactions between two surfaces, rutile is more reactive and produces more stable adsorbates.

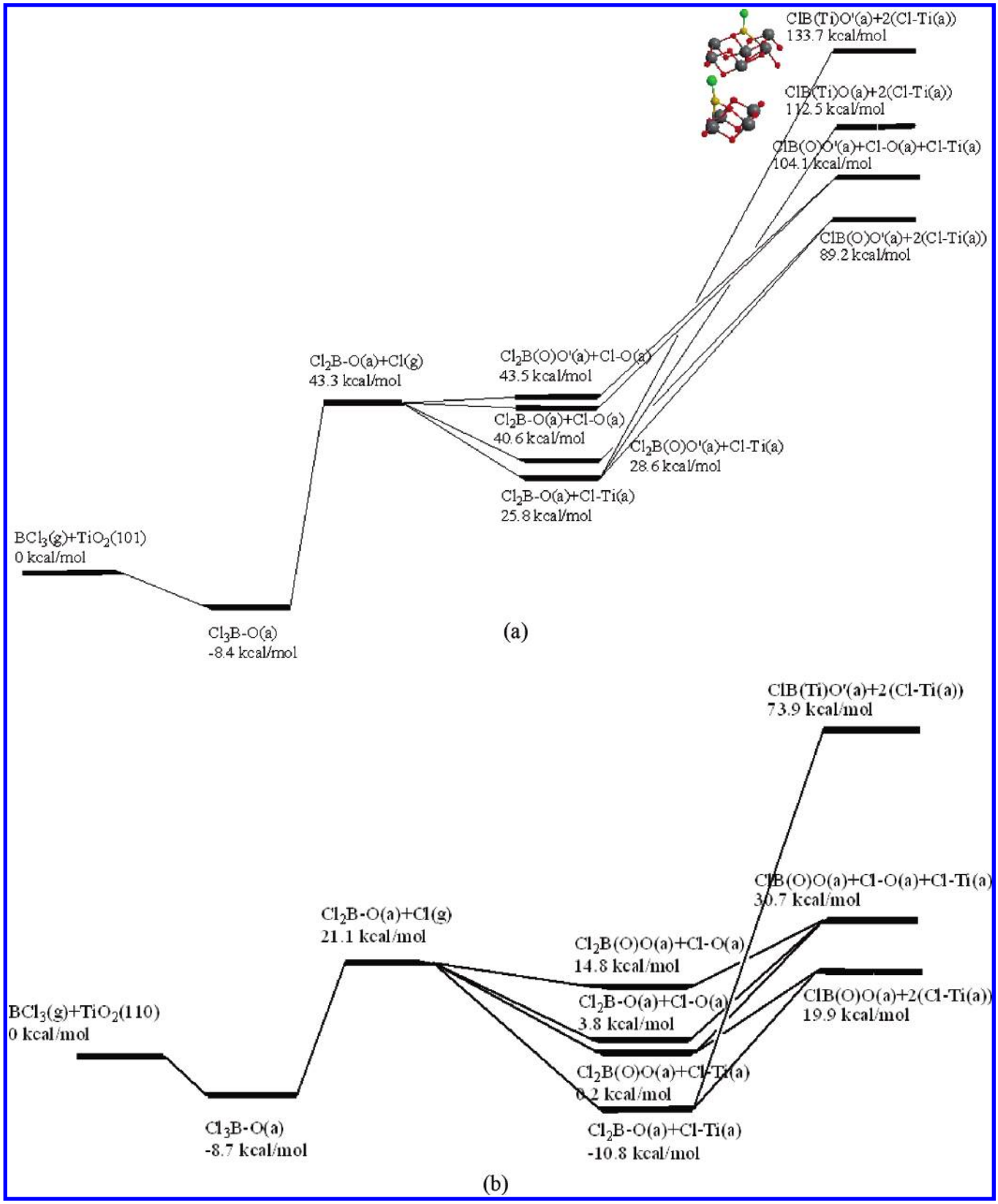

Figure 9. Potential energy surface of BClx on (a) TiO_2 anatase surface and (b) TiO_2 rutile surface.

Conclusion

This study investigates the adsorption and reaction of BCl_3 and its fragments on the TiO_2 anatase (101) and rutile (110) surfaces by first-principles calculations based on the DFT with GGA and the plane-wave method. The results show that the possible absorption configurations in both surfaces are very similar. Small differences were found due to the difference in the surface structures between anatase (101) and rutile (110). On the anatase surface the binding between B and Ti is negligibly weak. The potential energy surface shows that BCl_3 can be adsorbed on the O site on both surfaces, and starting from BCl_3, the formation of BCl_x(a) is endothermic. The BCl_x

reactions on the rutile surface have lower endothermicities than those on the anatase surface, reflecting the predicted stronger binding energies for BCl_x on the rutile surface. However, the energy barriers for the dissociation of BCl_x ($x = 1-3$) to smaller fragments are quite high. To functionalize TiO_2 with BCl_x species one needs plasma or UV irradiation, for example.

Acknowledgment. We are grateful for the use of CPU's at the National Center for High-Performance Computing in Hsinchu, Taiwan, supported by INER. One of the authors, J.-G.C., acknowledges the finical support from the Emerson Center Visiting Fellowship of Emory University. M.C.L. wants to acknowledge the partial support of this work by the MOE ATU Program and the National Science Council of Taiwan for a Distinguished Visiting Professorship and the Taiwan Semiconductor Manufacturing Co. for the TSMC Distinguished Professorship at the National Chiao Tung Unversity.

References and Notes

(1) Graetzel, M. *Nature* **2001**, *414*, 338.
(2) Asahi, R.; Morikawa, T.; Ohwaki, T.; Taga, Y. **2001**, *293*, 269.
(3) Fujishima, A.; Honda, K. *Nature* **1972**, *238*, 37.
(4) Hagfeldt, A.; Graetzel, M. *Acc. Chem. Res.* **200**, *33*, 269.
(5) Hagfeldt, A.; Graetzel, M. *Chem. Rev.* **1995**, *95*, 49.
(6) Kalyanasundaram, K.; Graetzel, M. *Coord. Chem. Rev.* **1998**, *177*, 347.
(7) O'Regan, B.; Graetzel, M. *Nature* **1991**, *353*, 735.
(8) Wang, J. H.; Lin, M. C. *Chem. Phys. Chem.* **2004**, *5*, 1615.
(9) Vittadini, A.; Selloni, A.; Rotzinger, F. P.; Graetzel, M. *J. Phys. Chem. B.* **2000**, *104*, 1300.
(10) Nilsing, M.; Lunell, S.; Persson, P.; Ojamae, L. *Surf. Sci.* **2005**, *582*, 49.
(11) Herman, G. S.; Dohnalek, Z.; Ruzycki, N.; Diebold, U. *J. Phys. Chem. B* **2003**, *107*, 2788.
(12) Kresse, G.; Hafner, J. *Phys. Rev. B* **1994**, *49*, 14251.
(13) Kresse, G.; Hafner, J. *Phys. Rev. B* **1993**, *47*, 558.
(14) Kresse, G.; Furthmuller, J. *Phys. Rev. B* **1996**, *54*, 11169.
(15) Kresse, G.; Furthmuller, J. *J. Comput. Mater. Sci.* **1996**, *6*, 15.
(16) Perdew, J. P.; Yang, Y. *Phys. Rev. B* **1992**, *37*, 785.
(17) Lee, C.; Yang, Y.; Parr, R. G. *Phys. Rev. B* **1988**, *37*, 785.
(18) Monkhorst, H.; Pack, J. *Phys. Rev. B* **1967**, *13*, 5188.
(19) Abrahams, S. C.; Bernstein, J. L. *Acta. Crystallogr, Sect. B* **1969**, *25*, 1233.
(20) Egashira, M.; Kawasumi, S.; Kagawa, S.; Seiyama, T. *Bull. Chem. Soc. Jpn.* **1978**, *51*, 3144.
(21) Wyckoff, R. W. G. *Crystal Structure*, 2nd ed.; Wiley: New York, 1964; Vol. 1.
(22) Goniakowski, J.; Gillan, M. J. *Surf. Sci.* **1996**, *350*, 145.
(23) Philip, J. D. L.; Harrison, N. M. *Phys. Rev. Lett.* **1998**, *80*, 762.
(24) Frisch, M. J. T. G. W.; Schlegel, H. B.; Scuseria, G. E.; Robb, M. A.; Cheeseman, J. R.; Zakrzewski, V. G.; Montgomery, J., J. A.; Stratmann, R. E.; Burant, J. C.; Dapprich, S.; Millam, J. M.; Daniels, A. D.; Kudin, K. N.; Strain, M. C.; Farkas, O.; Tomasi, J.; Barone, V.; Cossi, M.; Cammi, R.; Mennucci, B.; Pomelli, C.; Adamo, C.; Clifford, S.; Ochterski, J.; Petersson, G. A.; Ayala, P. Y.; Cui, Q.; Morokuma, K.; Malick, D. K.; Rabuck, A. D.; Raghavachari, K.; Foresman, J. B.; Cioslowski, J.; Ortiz, J. V.; Stefanov, B. B.; Liu, G.; Liashenko, A.; Piskorz, P.; Komaromi, I.; Gomperts, R.; Martin, R. L.; Fox, D. J.; Keith, T.; Al-Laham, M. A.; Peng, C. Y.; Nanayakkara, A.; Gonzalez, C.; Challacombe, M.; Gill, P. M. W.; Johnson, B.; Chen, W.; Wong, M. W.; Andres, J. L.; Gonzalez, C.; Head-Gordon, M.; Replogle, E. S.; Pople, J. A. *Gaussian03*; Gaussian, Inc.: Pittsburgh, PA, 2003.